Notch Filter Design Based on Two-Frequency Bode Diagram for Elastic Vibration Depression of Magnetically Suspended High-Speed Rotor

Wei Tong Fang Jiancheng
School of Instrumentation Science & Opto-electronics Engineering
Beijing University of Aeronautics and Astronautics
Beijing, China, 100083
weitong3000@sina.com

***Abstract*– In control moment gyroscope (CMG) based on magnetically suspended rotor (MSCMG), owing to wide controller bandwidth required by nutation stability at high rotational speed, bending mode between disk and axis of rotor with I-shaped configuration becomes unstable and tends to self-exciting vibration within the range of rotor speed. This elastic vibration can be depressed through adopting notch filter (NF) in original controller of active magnetic bearing (AMB), but NF design is still an issue since high-speed flat rotor features strong gyroscopic effect and coupling radial motions. By introducing complex representation, four DOFs (degrees of freedom) of dynamic model of magnetically suspend rotor considering unstable first-order bending mode is converted into single variable form without changing poles and stability. An illustrative and robust method of two-frequency Bode diagram is proposed to analyze elastic mode stability. Correction angle requirements of bending mode at various rotor speeds are summarized and parameters including NF grade, center frequency and pole damp are designed optimally. Employing the optimized notch filter, elastic vibration amplitude of statically suspended rotor of MSCMG was attenuated by -50.0dB comparing to original and the rotor is robustly stable within the entire speed range up to 20000r/min.**

***Index Terms* – Control moment gyroscope, Magnetic bearing, Elastic vibration depression, Two-frequency Bode diagram, Notch filter.**

I. INTRODUCTION

Control moment gyroscope (CMG) is a key actuator of attitude control system of large spacecrafts such as space stations, agile satellites and so on. To eliminate bearing friction and reduce unbalance force, magnetic bearings are implemented for high-speed rotor supporting of CMG, which is named magnetically suspended CMG (MSCMG) and has shown remarkable strengthens including high precision and long life[1]. However, owing to wide bandwidth of AMB controller required by nutation stability at high rotor speed[2], and relatively lower frequency of bending mode between disk and axis of rotor resulted from I-shaped configuration to achieve higher ratio of rotary inertia to rotor mass, MSCMG rotor becomes unstable and resonates at first-order bending mode frequency even at zero rotor speed[3][4], and remains vibrating within the range of rotor speed.

To depress elastic vibration, many methods such as notch filter (NF)[3][4][5][6][7], LQ control[8][9], LPV (Linear Parameter Varying) control[10], H_∞ control[11] and so on have been supplied previously. NF is one of the most effective methods, except that NF parameter is still hard to design to satisfy stability requirements within entire rotor speed range. Existing open-loop design method utilizes classic Bode or Nyquist diagram to determine NF for approximately decoupled slender rotor system with weak gyroscopic effect[4][5][6][7], but it is not suitable for MSCMG's high-speed flat rotor system which features strong gyroscopic effect and can't be decoupled. The alternative close-loop design[3] or multi-variable status space method are lack of illustrative and robust property, so as to be unpopular for actually utilization.

This paper focuses on elastic vibration depression of MSCMG rotor-AMB system with strong gyroscopic effect. Precise dynamic model of elastic rotor considering first-order bending mode has been obtained according to author's previous work[3]. Using this model, a new method based on two-frequency Bode diagram is presented to design NF. The simulation and experimental results demonstrate that the designed NF depresses elastic resonation effectively.

II. DYNAMIC MODEL CONSIDERING FIRST-ORDER ELSTIC MODE[3]

Calculation results according to ANSYS analysis indicate that self-exciting vibration of MSCMG rotor results from first-order elastic mode and is characterized as the relative bending between disk and axis of I-shape rotor in side view (Fig. 1). Only considering this unstable bending mode and ignoring other elastic ones for simplicity, MSCMG rotor can be modeled as a two-body structure consisting of rigid disk and axis connected by two

*. This project is supported by Hi-tech Research and Development Program of China.

orthogonal angular spring-dashpots, which enable disk and axis to swing relatively in 2 DOFs without translation and spin (Fig. 2). If angular stiffness k_k and angular damp k_v of spring-dashpots are introduced, the dynamic model considering first-order elastic mode can be written as follows

$$\begin{cases} J_{1y}\ddot{\beta} - H_1\dot{\alpha} + J_{2y}\ddot{\beta}_2 - H_2\dot{\alpha}_2 - 2k_h l_m^2\beta = -2l_m l_s k_i k_s g_c\beta \\ J_{1x}\ddot{\alpha} + H_1\dot{\beta} + J_{2x}\ddot{\alpha}_2 + H_2\dot{\beta}_2 - 2k_h l_m^2\alpha = -2l_m l_s k_i k_s g_c\alpha \\ J_{2y}\ddot{\beta}_2 - H_2\dot{\alpha}_2 - k_k(\beta-\beta_2) - k_v(\dot{\beta}-\dot{\beta}_2) = 0 \\ J_{2x}\ddot{\alpha}_2 + H_2\dot{\beta}_2 - k_k(\alpha-\alpha_2) - k_v(\dot{\alpha}-\dot{\alpha}_2) = 0 \end{cases} \quad (1)$$

where α, β and α_2, β_2 are tilt angle of axis and disk relative to AMB stator respectively, H_1 and H_2 angular momentum of axis and disk respectively, J_{1x}=J_{1y} and J_{2x}=J_{2y} radial moment of inertia of axis and disk respectively, k_s sensitivity of AMB displacement sensor, k_i and k_h current stiffness and displacement stiffness of AMB electromagnet respectively, l_m and l_s distance from electromagnet and displacement sensor to rotor center respectively. g_c denotes transform operator of AMB controller from input to output in time domain, i.e. $L[g_c\alpha]$=$g_c(s)\alpha(s)$, where $g_c(s)$ and $\alpha(s)$ are *Laplace* transformation of g_c and α respectively. Supposing g_c has been configured to be able to stabilize translation and whirling motion (precession and nutation) of rigid body, stability of first-order elastic mode can be analysis and NF parameters can be design based on above dynamic model.

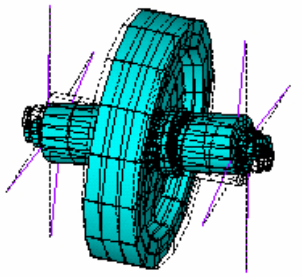

Fig. 1 The first-order elastic modal type of MSCMG rotor

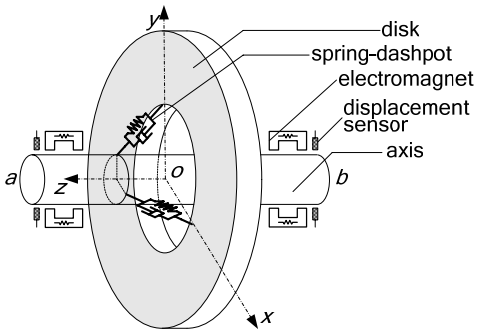

Fig. 2 Mechanic model of MSCMG rotor considering first-order elastic mode

III. ELASTIC MODE STABILITY ANALYSIS BASED ON TWO-FREQUENCY BODE DIAGRAM

For MSCMG rotor, H_2 is considerable large due to flat type and high speed, which causes strong gyroscopic effect. It is impossible to decouple radial motions of such a rotor to use classic Bode diagram for NF design directly according to equation(1). However, in order to realize illustrative and robust design, the original system will be converted to a single variable model. Then the extended two-frequency Bode diagram is presented to analyze elastic mode stability, which is the foundation of NF parameters design.

A. Single Variable Equivalent Form of Dynamic Model

Define J_{1rr}=J_{1x}=J_{1y}, J_{2rr}=J_{2x}=J_{2y}, φ=α+$j\beta$ and φ_2=α_2+$j\beta_2$, where j is the imaginary unit. According to equation(1), we have

$$\begin{cases} J_{1rr}\ddot{\varphi} - jH_1\dot{\varphi} + J_{2rr}\ddot{\varphi}_2 - jH_2\dot{\varphi}_2 - 2k_h l_m^2\varphi = -2l_m l_s k_i k_s g_c\varphi \\ J_{2rr}\ddot{\varphi}_2 - jH_2\dot{\varphi}_2 = k_k(\varphi-\varphi_2) + k_v(\dot{\varphi}-\dot{\varphi}_2) \end{cases} \quad (2)$$

By eliminating $\varphi(s)$ and $\varphi_2(s)$ in *Laplace* transformation result of equation (2), we get

$$J_{1rr}s^2 - jH_1 s + \frac{(J_{2rr}s^2 - jH_2 s)(k_k + k_v s)}{J_{2rr}s^2 + (k_v - jH_2)s + k_k} - 2k_h l_m^2 = -2l_m l_s k_i k_s g_c(s) \quad (3)$$

So equation (1) can be converted into a feedback control system as Fig. 3. The relevant equivalent controlled object and equivalent controller are:

$$g_{oeff}(s) = \frac{1}{J_{1rr}s^2 - jH_1 s + \frac{(J_{2rr}s^2 - jH_2 s)(k_k + k_v s)}{J_{2rr}s^2 + (k_v - jH_2)s + k_k} - 2k_h l_m^2} \quad (4)$$

$$g_{ceff}(s) = 2l_m l_s k_i k_s g_c(s) \quad (5)$$

Equivalent open loop transfer function (TF) with complex coefficients is:

$$g_{OL}(s) = g_{oeff}(s)g_{ceff}(s) \quad (6)$$

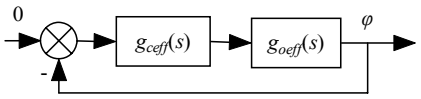

Fig. 3 Block diagram of equivalent feedback control system

By above complex transformation, the gyroscopic couple system with four variables is converted into a single variable system with complex coefficients without changing poles and stability, and can be analyzed using linear control theory only considering complex coefficients additionally.

B. Stability Analysis Criterion of Two-Frequency Bode Diagram

Classic control theory describes single variable system frequency characteristics (FC) by Bode diagram including logarithm amplitude frequency characteristics (AFC), $L(\omega)$, and logarithm phase frequency characteristics (PFC), $\phi(\omega)$. Since FC of TF with real coefficients is symmetric about zero frequency, only FC in positive frequency is concerned. With respect to g_{OL}(s) with complex coefficients, $g_{OL}(-j\omega)$ and $g_{OL}(j\omega)$ are not symmetric about zero frequency, so Bode diagram of g_{OL}(s) comprises not only $L(\omega)$ and $\phi(\omega)$

of $g_{OL}(j\omega)$, positive frequency Bode diagram, but also $L(-\omega)$ and $\phi(-\omega)$ of $g_{OL}(-j\omega)$, negative frequency Bode diagram, which are named as two-frequency Bode diagram in general.

Being identical to Bode diagram stability criterion, two-frequency Bode diagram can be used to determine stability of single-variable linear system with complex coefficients, if negative FC is considered additionally. The criterion is: Define Q as number of open loop poles with positive real part, L_{N+} and L_{P+} as ω zone where $L(-\omega)>0$ and $L(\omega)>0$ respectively, N_{n+} and N_{n-} as forward and backward cross-over times of $\phi(-\omega)$ through $(2k+1)\pi$ line within L_{N+}, N_{p+} and N_{p-} as forward and backward cross-over times of $\phi(\omega)$ through $(2k+1)\pi$ line within L_{P+} (k=0,1,2…), and $N=N_{n+}+N_{p+}-N_{n-}-N_{p-}$ as total cross-over times, Z as number of close loop poles with positive real part, thus $Z=Q-N\geq 0$, and close loop stable equals to $Z=0$.

C. Elastic Mode Stability Determination Based on Two-Frequency Bode Diagram

Above all, Q value must be known. Open-loop poles of $g_{OL}(s)$ with positive real part comes from $g_{oeff}(s)$ only, which can be calculated by the equation as follows

$$J_{1rr}s^2 - jH_1 s + \frac{(J_{2rr}s^2 - jH_2 s)(k_k + k_v s)}{J_{2rr}s^2 + (k_v - jH_2)s + k_k} - 2k_h l_m^2 = 0 \quad (7)$$

According to the parameters of MSCMG prototype, which are shown in table 1, open-loop poles at different rotor speed are calculated and plotted in Fig. 4, where low frequency poles are relevant to rigid modes (precession and nutation), and high frequency poles relevant to backward whirl (BW) and forward whirl (FW) of elastic mode. Evidently, $Q=1$ if rotational speed F_r is lower than F_{r0} and $Q=0$ if F_r is higher than F_{r0}, where $F_{r0}=115$Hz relevant to the MSCMG prototype.

Table 1 MSCMG prototype parameters

Parameter	Value	Parameter	Value
m	13.3 kg	k_i	404N/A
J_{rr}	0.062 kgm^2	k_h	2084600N/m
J_z	0.096 kgm^2	k_w	0.165A/V
l_m	0.06825m	k_s	0.073V/μm
l_s	0.10275m		

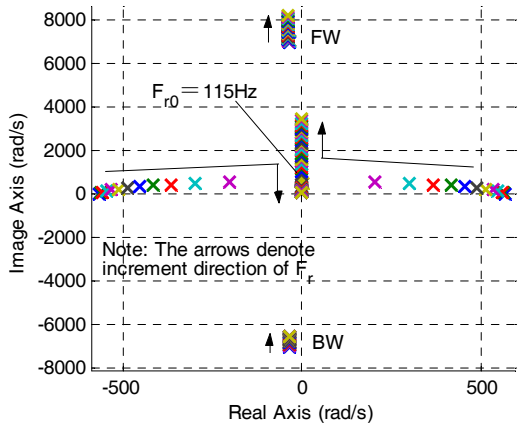

Fig. 4 Open-loop poles of magnetically suspended elastic rotor system at rotor speed from 0 to 400Hz

Two-frequency Bode diagram of magnetically suspended rotor at $F_r=0$Hz and 400Hz can be seen in Fig. 5a and 5b respectively, where negatively FC is flipped to positive field, and upward and downward arrows in PFC denote half a positive or negative cross-over respectively. Stability determination results of AMB-rotor system are

1) When $F_r=0$Hz, $Q=1$, $N=1+1-1.5-1.5=-1$, $Z=1-(-1)=2$, and the system is unstable (Fig. 5a).

2) When $F_r=400$Hz, $Q=0$, $N=1+0-1.5-1.5=-2$, $Z=0-(-2)=2$, so the system is still unstable (Fig. 5b). It is similar when $0<F_r<400$Hz.

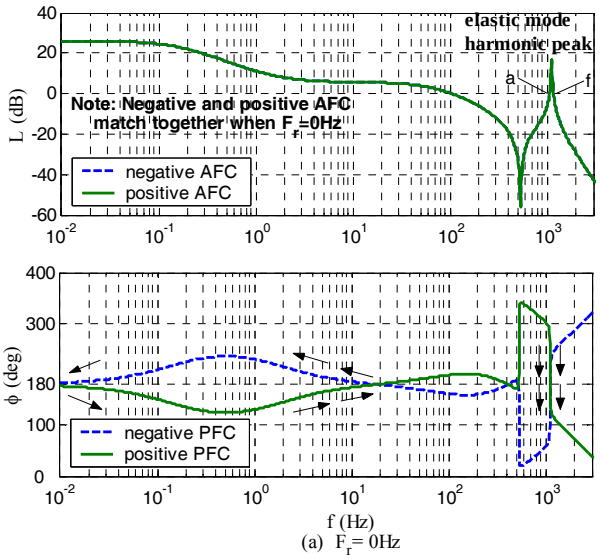

(a) $F_r=0$Hz

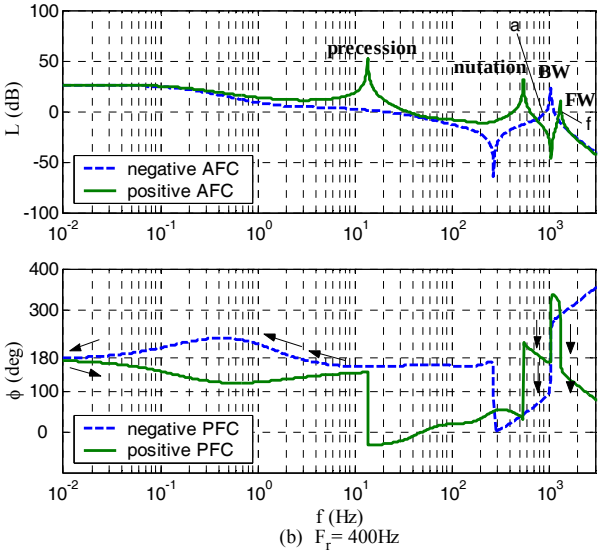

(b) $F_r=400$Hz

Fig. 5 Two-frequency Bode diagram of magnetically suspended rotor at different rotational speed

Define L_{B+} and L_{F+} as ω zone where $L(-\omega)>0$ in BW harmonic peak and $L(\omega)>0$ in FW harmonic peak respectively in the two-frequency diagram. Since low frequency zone of two-frequency Bode diagram which covers precession and nutation has $Z=0$, instability must result from cross-over in L_{B+} and L_{F+} due to high

frequency phase lag of AMB control, i.e., precession and nutation are stable, while BW and FW unstable at whole range of rotational speed, which conforms to stability determination results using close-loop locus[3].

D. Stability Margin Analysis

Define Left limit of L_{B+} as point *a*, right limit of L_{F+} as point *f*, relevant frequency as f_a and f_f, phase margin $\gamma_B(\gamma_F)$ can be described as minus value of the minimum leading angle required to eliminate BW(FW) cross-over at frequency of $f_a(f_f)$, which are written as follows:

$$\begin{cases} \gamma_B = \angle g_{OL}(j2\pi f_a) - 180^\circ \\ \gamma_F = \angle g_{OL}(j2\pi f_f) - 180^\circ \end{cases} \tag{8}$$

Positive, zero and negative phase margin denote stable, critical stable and unstable respectively, and the larger absolute value, the more stable or unstable. $\gamma_B(\gamma_F)$ with respect to $f_a(f_f)$ at different rotational speed is shown in Fig. 6. It can be seen that γ_B and γ_F are negative within the whole rotation speed range, and elastic mode is the most unstable when F_r=0Hz. It also can be seen that BW is always more unstable than FW since BW frequency decreases and more close to control bandwidth when rotor ramps up.

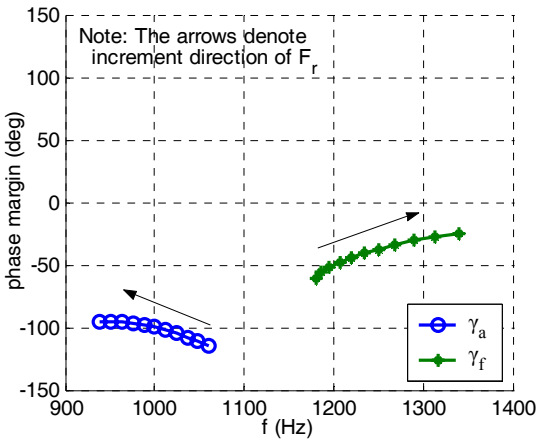

Fig. 6 Phase margin of BW and FW at various rotational speed

IV. NOTCH FILTER DESIGN

According to phase margin graph of elastic mode, BW and FW modes will restore to be stable if negative and positive PFC are leaded $|\gamma_a|$ in f_a and $|\gamma_f|$ in f_f respectively without changing L_{B+} and L_{F+}. Using minimum phase correction, PFC of correction segment is oddly symmetric about zero frequency, and above leading angle requirement will all flip to positive frequency and will be: $|\gamma_a|$ lag in f_a and $|\gamma_f|$ leading in f_f. Evidently, PFC of NF satisfies this requirement very well, so that NF with solid parameters can depress elastic vibration within given rotational speed range. TF of typical NF is

$$g_{nf}(s) = \frac{s^2 + \omega_z^2}{s^2 + 2\zeta_p \omega_z s + \omega_z^2} \tag{9}$$

where $\omega_z=2\pi f_z$, f_z and ζ_p are center frequency and pole damp of NF respectively. How to design NF grades n, f_z and ζ_p will be discuss as follows.

A. *n* Design

NF grades requirement depends on maximum phase leading angle required comparing to θ_{max}, maximum leading angle of NF, i.e.

$$n = \text{int}\{[\max(|\gamma_a|, |\gamma_f|) + \gamma]/\theta_{max} + 1\} \tag{10}$$

where "int" means getting round number, γ given design destination of phase margin. Usually θ_{max}=70°, γ=10°. According to Fig. 6, obviously n=2.

B. f_z Design

When F_r=0Hz, which means the rotor suspended statically without spinning, NF depresses vibration by eliminating harmonic peak through rejection band, so f_z must be identical with or a little lower than harmonic peak frequency in Fig. 5a, which is shown below

$$f_z = f_{b0} = f_{e0} \tag{11}$$

According to Fig. 5a, we can select $f_z = f_{b0} = 1117$Hz.

C. ζ_p Design

ζ_p design is the most important since NF correction angle depends on ζ_p value. After divided by the grade n =2, and reversing the right part, phase margin from Fig. 6 is compared to NF PFC and normalization result is shown in Fig. 7. It can be seen that FW stability or statically suspension stability requires less ζ_p, while BW stability at maximum rotational speed (BW_{max} stability) require the largest ζ_p. Since NF will reduce nutation stability owing to its phase lag at nutation frequency, and the higher ζ_p the larger phase lag, ζ_p should be minimized to decrease influence to nutation stability while guarantee BW and FW phase margin. This optimization needs only to be done at maximum rotational speed, since BW_{max} stability requires the largest phase leading angle.

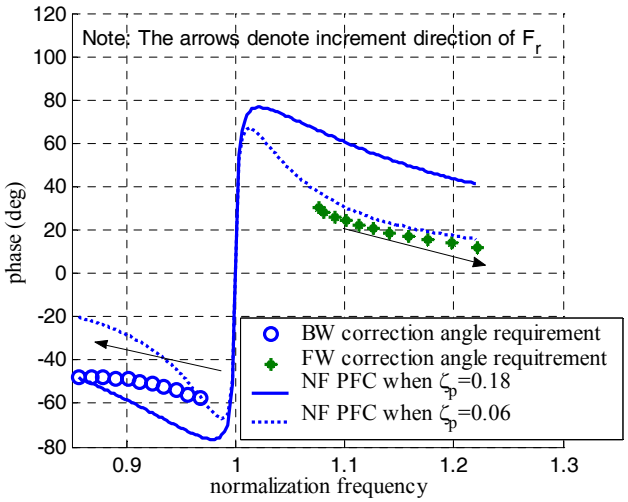

Fig. 7 Normalization of phase requirement and NF frequency characteristics

To minimize ζ_p requirement, magnitude decaying characteristics of NF should be considered. If NF is

placed in AMB controller, left limit of L_{B+} will move right a bit and phase leading requirement decreases, which also decrease ζ_p requirement. For arbitrary ζ_p, TF with NF at $F_r=F_{r\max}$ is

$$g_{OL1}(s)\big|_{F_r=F_{r\max}} = g_{OL}(s)\left(\frac{s^2+2\zeta_z\omega_z s+\omega_z^2}{s^2+2\zeta_p\omega_z s+\omega_z^2}\right)^n\Bigg|_{F_r=F_{r\max}} \quad (12)$$

where f_z and n have been determined. Supposing f_a move right to f_{a1} when $\zeta_p=\zeta_{p0}$, and phase margin of BW_{max} is just right γ required, the new open-loop TF can be expressed as follows

$$g_{OL1}(s)\big|_{s=-j2\pi f_{a1},\zeta_p=\zeta_{p0}} = e^{j(\pi+\gamma)} \quad (13)$$

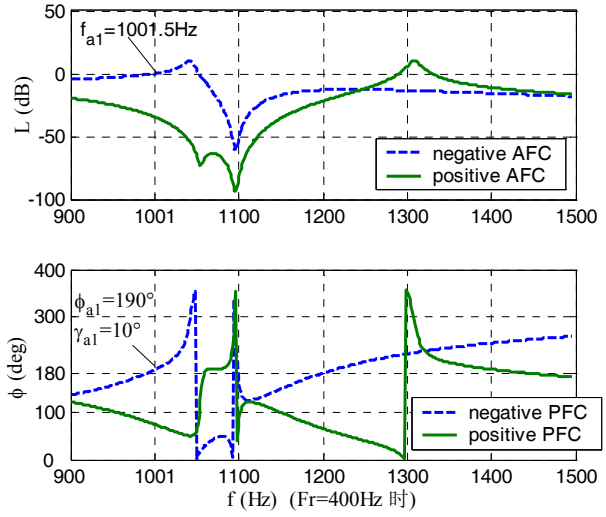

Fig. 8 Two-frequency Bode diagram of magnetically suspended rotor with NF

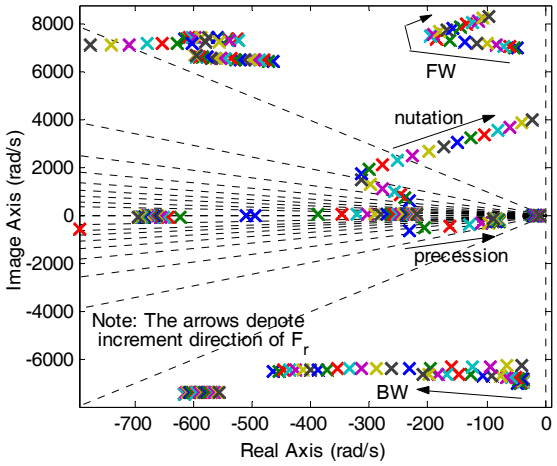

Fig. 9 Close-loop locus of magnetically suspended rotor with NF（F_r =0～400Hz）

According to equation(13), ζ_{p0} and f_{a1} can be calculated and the results are f_{a1}=1001.5Hz and ζ_{p0}= 0.1061. Comparing to ζ_p=0.18, phase lag of two-grade optimal NF at 642Hz (nutation frequency relevant to F_r =400Hz) decreases from 35° to 21°, which will reduce influence to nutation stability significantly. Two-frequency Bode diagram relevant to F_r=400Hz is shown in Fig. 8, where phase margin of BW is γ=10° exactly. The close-loop locus of AMB-rotor system with NF is shown in Fig. 9, and it can be seen that BW and FW are stable within entire rotational speed range.

V. EXPERIMENTAL RESULT

Fig. 10 MSCMG prototype

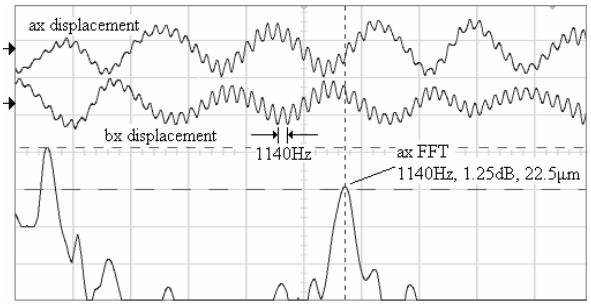

Fig. 11 Displacement signal of statically suspended rotor without NF (vertical axis 138μm/div, horizontal axis 5ms/div)

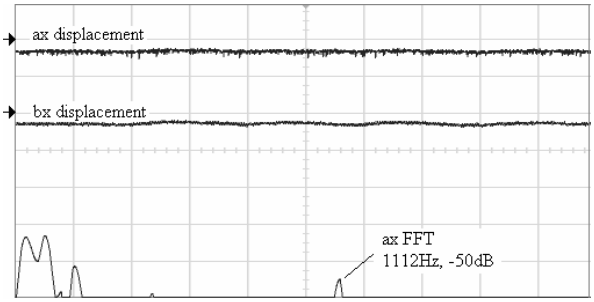

Fig. 12 Displacement signal of statically suspended rotor with NF (vertical axis 7μm/div, horizontal axis 5ms/div)

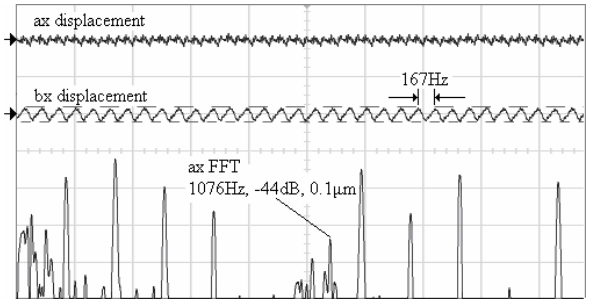

Fig. 13 Displacement signal of suspended rotor with NF at 10000r/min (vertical axis 28μm/div, horizontal axis 20ms/div)
Notes: Left arrows denote zero of signal. 0dB equals amplitude of 20μm

The designed NF is test using MSCMG prototype

developed by Beijing University of Aeronautics and Astronautics, the parameters of which are shown in table 1. Actual NF parameters are n=2, f_z=1110Hz and ζ_p=0.084, which are very close to the designed NF. Firstly, MSCMG rotor was statically suspended without NF. The rotor vibrated violently, *ax* and *bx* displacement signals and FFT spectrum shown in Fig. 11. The 1140Hz segment had an amplitude of 22.5μm (1.25dB). After inserting the NF, self-exciting vibration was depressed to -50dB right now and the magnetically suspended rotor restored to be stable (Fig. 12). Then the rotor was ramped up to 10000r/min. The detected vibration is BW segment at 1076Hz, but its displacement was only 0.1μm (-44dB, Fig. 13). The fluctuation of 167Hz in the signal results from not elastic mode but unbalance and was stable.

VI. CONCLUSIONS

By introducing complex coefficients, four DOFs of close-loop rotor dynamical model of MSCMG is converted into equivalent single variable form. Afterward, a novel method based on two-frequency Bode diagram is proposed to analyze flexible rotor stability with strong gyroscopic effect. Correction angle requirements of elastic mode at various rotor speed are summarized and NF parameters including grades, center frequency and pole damp are designed optimally. Employing the designed notch filter, elastic mode amplitude was attenuated by -50.0dB comparing to original and MSCMG rotor is robustly stable within entire speed range up to 20000r/min. It can be concluded that elastic mode loses stability owing to high-frequency lag of AMB controller, and notch filter with fixed parameters can stabilize elastic bending mode because it has phase-frequency characteristics satisfying phase-leading requirements for bending mode stabilization at different rotor speeds, and shown minor influence to other mode due to very narrow action range. The simulation and experimental results demonstrate that the designed NF depresses elastic mode self-exciting vibration effectively, which verifies efficiency of two-frequency Bode diagram and NF design method.

ACKNOWLEDGEMENT

The authors would like to thank Prof. Li Jichen, Prof. Liu Gang and Dr. Chen Dong *et al*. for their help in carrying out all the experiments.

REFERENCES

[1] Roser X., Sghedoni M. Control Moment Gyroscopes (CMG's) and their Application in Future Scientific Missions. Proceedings of Third International Conference on Spacecraft Guidance, Navigation and Control Systems, Noordwijk, Netherlands, Nov. 26-29, 1996: 523-528

[2] Wei Tong, Fang Jiancheng. A Phase-Leading Compensation Method Used to Control Nutation of Magnetically Suspended Rotor in Control Moment Gyroscope. Fifth International Symposium on Instrumentation and Control Technology (ISICT). Beijing, China. Oct., 24-27, 2003: 810-813

[3] Wei Tong, Fang Jiancheng. Dynamics Modeling and Vibration Suppression of High-Speed Magnetically Suspended Rotor Considering First-Order Elastic Natural Vibration. Proceedings of the 9th International Symposium on Magnetic Bearings. Lexington, Kentucky, Aug. 3-6, 2004: No.97

[4] Timothy P. D., Gerald V. B., Ralph H. J., et al. Magnetic Bearing Controller Improvements for High Speed Flywheel System. Glenn Research Center, NASA/TM-2003-212733, 2003

[5] Makoto Ito, Hiroyuki Fujiwara, Osami Matsushita. Evaluation of Stability Margin of Active Bearing Control System Combined with Several Filters. Proceedings of the 9th International Symposium on Magnetic Bearings. Lexington, Kentucky, Aug. 3-6, 2004: No. 95

[6] Hiroyuki Fujiwara, Koji Ebina, Makoto Ito, et al. Control of Flexible Rotors Supported by Active Magnetic Bearings. Proceedings of the 8th International Symposium on Magnetic Bearings. Mito, Japan, Aug., 26-28, 2002: 145-150

[7] Hiroyuki Fujiwara, Osami Matsushita and Hiroki Okubo. Stability Evaluation of High Frequency Eigen Mode for Active Magnetic Bearing Rotors. Proceedings of the 7th International Symposium on Magnetic Bearings. ETH Zurich, Switzerland, Aug. 23-25, 2000: 83-88

[8] Yuichi Nakajima, Mitsuhiro Ichihara, Takahito Sagane, et al. A New Modeling Technique and Control System Design of Flexible Rotor Using Active Magnetic Bearings for Motion and Vibration Control. Proceedings of the 9th International Symposium on Magnetic Bearings. Lexington, Kentucky, Aug. 3-6, 2004: No. 52

[9] Hideo Shida, Mitsuhiro Ichihara, Kazuto Seto, et al. Motion and Vibration Control of Flexible Rotor Using Magnetic Bearings. Proceedings of the 8th International Symposium on Magnetic Bearings. Mito, Japan, Aug., 26-28, 2002: 381-387

[10] Stephen Mason, Panagiotis Tsiotras and Paul Allaire. Linear Parameter Varying Controllers for Flexible Rotors Supported on Magnetic Bearings. Proceedings of the 6th International Symposium on Magnetic Bearings. Cambridge, Unite States, Aug. 5-7, 1998: 341-351

[11] Tomoaki Takami, Michihiro Kawanishi and Hiroshi Kanki. Advanced Control for Active Magnetic Bearing. Proceedings of the 8th International Symposium on Magnetic Bearings. Mito, Japan, Aug., 26-28, 2002: 439-444